Author(s): Patil, Ajay B.; Thalmann, Nicole; Torrent, Laura; Tarik, Mohamed; Struis, Rudolf P. W .J.; Ludwig, Christian

Title: Surfactant-based enrichment of rare earth elements from NdFeB magnet e-waste : Optimisation of cloud formation and rare earths extraction
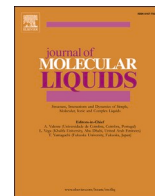
Year: 2023

Version: Published version

Please cite the original version:

Patil, A. B., Thalmann, N., Torrent, L., Tarik, M., Struis, R. P. W. .., & Ludwig, C. (2023). Surfactant-based enrichment of rare earth elements from NdFeB magnet e-waste : Optimisation of cloud formation and rare earths extraction. Journal of Molecular Liquids, 382, Article 121905. https://doi.org/10.1016/j.molliq.2023.121905

ELSEVIER

Check for updates

Surfactant-based enrichment of rare earth elements from NdFeB magnet e-waste: Optimisation of cloud formation and rare earths extraction

Ajay B. Patil [a,b,1,2,*], Nicole Thalmann [a,c,3], Laura Torrent [a], Mohamed Tarik [a,4], Rudolf P.W. J. Struis [a,b,*], Christian Ludwig [a,b]

[a] Chemical Processes and Materials Research Group, Energy and Environment Research Division, Paul Scherrer Institute (PSI), Forschungsstrasse, 111, CH-5232, Villigen PSI, Switzerland
[b] École Polytechnique Fédérale de Lausanne (EPFL), ENAC IIE GR-LUD, CH-1015 Lausanne, Switzerland
[c] Ecological Systems Design, Institute of Environmental Engineering (IFU) ETH Zurich, John-von-Neumann-Weg 9, CH-8093 Zurich, Switzerland[5]

ABSTRACT

Appropriate waste and resource management are essential for a sustainable circular economy with reduced environmental impact. With critical resources, e-waste may serve as indirect raw material. For example, with NdFeB permanent magnets, Neodymium (Nd) and the co-present Dysprosium (Dy) are critical rare earth elements (REEs). However, there exists no economically viable technology for recycling them from electronic waste (e-waste). Here, a method is presented based on cloud point extraction (CPE). The work involves basic complexation chemistry in a cloud medium with pure REE salts, as well as, with real NdFeB-magnets (nearly 28% REE content by weight) from an old hard disk drive (5.2 g magnet in a 375 g HDD). High extraction efficiency (>95%) was achieved for each REE targeted (Nd, Dy, Praseodymium (Pr)). With the magnet waste, the cloud phase did hardly contain any Nickel (Ni), Cobalt (Co), or Boron (B), but some Aluminium (Al) and Iron (Fe). Dynamic light scattering results indicated aggregation of ligand-surfactant micelles with the cloud phase. The preconcentrated products can be used for new Nd magnet manufacturing or further enriched using established transition metal removal techniques. Reuse of solvent, low chemical inventory demand, and using non-inflammable, non-volatile organic extractants promise safe large-scale operation, low process costs, and less environmental impact than using hydrometallurgical methods used with urban or primary mining.

1. Introduction

Our scientific and technological growth is undergoing in two significant directions. On the front end, we are witnessing the advent of smart, green and hybrid electronic technologies. On the back end, this resulted in a by-product of 44.7 million metric tonnes of e-waste in 2016 with 6.1 kg/person waste generation [1,2]. These types of devices and technologies rely on essential raw materials such as Rare Earth Elements (REEs). REEs comprise the group of 17 metals (Sc, Y, La-Lu) that make our devices faster, smarter and with smaller sizes and lower energy

requirements [3–5]. However, their increased use and resulting end-of-life e-waste is now the most considerable growing fraction of the municipal solid waste stream with only a 20% recycling rate [6–8]. Nowadays, established recycling mainly concerns dismantling and crushing the e-waste in smaller volumes. Except for plastic, glass and ferrous metals, most of the other by-products and secondary wastes, including REEs, are landfilled or incinerated, hereby, producing also more greenhouse gas. There is also a growing concern about the sustainable supply of critical REEs. Following the guidelines from the Minamata and Basel conventions and those from the Paris Agreement, it

is now globally mandatory to process the generated e-waste within the state boundaries and to decrease the landfilling rates [1,7]. Therefore, it is essential to develop new recovery processes and alternative supply chains from secondary resources [3–8].

The significant process challenge in the recycling of raw materials is the separation of the REEs due to their similar physical and chemical properties (lanthanide contraction effect), heterogeneous nature plus impurities of the waste feedstock, and the dilute REE content in waste streams. REE mining activities also involve radioactive by-products, tailings, and substantial amounts of acidic feeds [9–13]. Therefore, conventional mining techniques cannot be used directly for recycling applications [14–19].

Researchers are focusing on different secondary waste feedstock for metal recovery. Lighting devices, magnets, and battery materials possess relatively high REE contents that could be exploited. Magnets are one of the most revolutionalised commodities by REEs. Therefore, their increasing use is eventually giving rise to increased e-waste streams. The presence of REEs in hard disc drives (HDDs), cellphones, wind turbines, and hybrid cars can generate substantial amounts of such e-waste in the near future [20–25]. The importance of REEs recycling technologies is evident from the large number of papers published recently in this area of research [26–35].

The NdFeB magnet has an impressive content of REEs (28–30 wt%) and therefore can serve as a good secondary feed for the REEs recovery. A substantial amount of these NdFeB magnets are used in HDDs and are available in the end-of-life value chain for REE recovery. Nearly 112,000 tons of NdFeB magnets were produced in 2012 on a global scale that was used in the production of nearly 500 million units of HDDs in the year 2015. With growing data storage demand, HDDs are expected to be the major fraction of global e-waste, amounting to 75 million tons by the year 2030. A typical HDD contains nearly 5.2 g of magnet in a 375 g HDD. Out of this, nearly 1.46 g is the amount of REEs per HDD [36–38]. Therefore, with the expected growth of the reusable REE content in the end-of-life HDDs, their value chain needs to be harnessed from the circular economic perspective for reducing the substantial environmental impact of our data storage activities.

The indispensable REEs separation can be achieved by choosing appropriate hydrometallurgical conditions and suitable ligands. REEs are hard acids as per the Hard-Soft Acid-Base (HSAB) theory [39]. Different extractants with organophosphorus and carbonyl functionality have been proposed and evaluated for the recovery of actinides and lanthanides from acidic feeds, usually from the mining feedstock [17–19,39]. Liquid-liquid extraction is typically the method of choice due to its high throughput, low energy requirements, and ease of operations compared to electrochemical and thermal methods. However, such extractions usually have the issue of large (hence costly and secondary waste producing) extracting agent inventory/stock requirements in rare earth separation work [15,16]. Thus, green extraction methods are required to enhance the sustainability and environmental friendliness of the rare earth comprising *f*-block elements [39–44].

Cloud point extraction (CPE) has emerged as the promising, affordable and green technique to recover metals from different feedstock under optimised conditions. In this method, a non-ionic surfactant and a ligand in a miscible solution are transformed into a surfactant-rich ("cloud") phase by heating and carrying the metal ions of interest along with it [45]. Such distribution is due to the formation of micelles with the surfactant in the colloidal solution, as the hydrophobic ends of the ligand molecules are on the outside of the ligand-REE complex. CPE may also separate RE cations from mostly less-valent impurities [44,46–52]. CPE has been used to determine and quantify REEs in trace impurity levels [53,54]. In the literature, CPE was performed in a perchlorate medium. But, perchlorate medium is unsuitable for large-scale separation operations due to the possibility of shock detonation and its pyrophoric nature [44]. To our knowledge, the CPE method has not been tried for e-waste recycling before.

This paper describes a new method by which permanent magnet e-

waste could be exploited for the recovery of REEs. The process development and optimisation had been carried out with pure REE salts, as well as, with NdFeB magnets taken from end-of-life HDDs. We used a surfactant-based method with less organic extractant and diluent inventory to have a lower environmental impact as compared to conventional hydrometallurgical methods [23,26–30].

2. Material and methods

2.1. Instruments and apparatus

The elemental composition of REE in waste and pure samples were analysed with Inductively Coupled Plasma Spectroscopy (ICP-OES, Spectro Arcos, Germany). Calibration solutions made from a multi-element standard solution containing 16 REEs except for the radioactive Pm (Fluka, Germany) with concentrations ranging from 0 to 10 mg/L were used for the quantification. The number of metals in the cloud phase was calculated using the difference between the homogeneous starting/control solution with that of the final aqueous phase measured with ICP-OES.

In the extraction experiment, 15 mL Cellstar-Centrifuge sample tubes (polypropylene (PP), graduated, conical bottom, sterile) were used. Teflon tape from Angst and Pfister (USA) was used to prevent leakage during heating in a water bath. Sample drying was done in a Heraeus VT 5050EK oven at 90 °C. All solutions were prepared in ultrapure Milli-Q water (resistivity of 18.2 MΩ) from a Sartorius Stedim Biotech Arium Pro-VF water purifier. All the experiments were performed in duplicates unless stated otherwise.

During all experiments - unless stated otherwise - all the PP tubes were pre-treated as described by Kumari et al. (2013) [44] to avoid the absorption of metal ions by the tube wall. Pre-treatment was done with two items of washing of 0.001 M HNO_3, followed by two items of washing of 0.001 M HCl, and five items of washing of Milli-Q before they were air-dried. Handy step pipettes (for amounts > 1 mL) and Eppendorf Research plus pipettes (≤1 mL) were used for the liquid reagents measurements. Mettler AE 240 and Mettler Toledo PR2003 scales were used to weigh solid materials. pH indicator strips (MColorpHas+^{TM}, pH 0.0–6.0) or the device ExStik (pH100) were used for the acidity determination in the pH range. Heidolph Reax 2000 shaker vortexer was used to homogenise the samples. Cloud point extraction experiments were done with a constant temperature shaker bath (CTSB) HT from Infors AG between 20 and 82 °C. It was used at a 60 RPM shaking speed. In some experiments, a temperature up to 95 °C was reached using a non-shaking thermostat from LAUDA E200. For centrifugation, the Hettich Universal 1200 instrument was used at > 3000 RPM.

A Malvern Nanoseries Zetasizer was used for the dynamic light scattering (DLS) measurements in the range of 50 – 75 °C. The demagnetisation of magnets was done using heat treatment at 950 °C using a tubular furnace from Heraeus instruments. It was then ground using a Fritsch pulverisette machine. The feed composition of magnet e-waste was determined by complete digestion using Multiwave 3000 microwave from Anton Paar.

2.2. Reagents

Tricapryl methyl ammonium chloride (Al336), sodium citrate dehydrate, citric acid, cerium nitrate hexahydrate, acetic acid, hydrochloric acid, bis (2-ethylhexyl) phosphate, nitric acid, potassium chloride, lanthanum nitrate hexahydrate, neodymium oxide, oxalic acid, and theonyl trifluoroacetone were procured from Aldrich Chemistry. Triton X100 was procured from Fluka. Sodium nitrate and sodium acetate were procured from Merck. *N,N′*-dimethyl-*N,N′*-dicyclohexyl-malonamide (DMDCMA) was prepared in-house using the method reported elsewhere [39].

The Neodymium nitrate and Dysprosium nitrate were prepared by converting respective oxides to nitrates and drying them. Dy- and Nd-

nitrate were prepared using 0.5 g of the pure Dy_2O_3 (white powder) and Nd_2O_3 (blueish powder) respectively. They were separately dissolved in TraceSELECT (ultra-high purity reagent) HNO_3 (10 mL for Dy and 1 mL for Nd). The resulting clear solution was then dried in the Heraeus oven at T = 90 °C for 5 days. The resultant powder of nitrate derivatives of Dy and Nd was used for further experiments.

The defined pH solutions were prepared using the stock solutions of 0.2 M potassium chloride (KCl), 0.2 M hydrochloric acid (HCl), 0.1 M citric acid ($C_6H_8O_7$) and 0.1 M trisodium citrate dihydrate ($C_6H_5O_7N$-a_3·$2H_2O$) (Table 1).

2.3. Digestion of magnet samples and analysis

Magnet powder was mixed with 10 mL HNO_3 or/and HCl and 5 mL Milli-Q water and digested in a high-pressure microwave unit (Multiwave 3000, Anton Paar, Austria) using a power of 800 W and a duration of 60 min. The samples were diluted in 1% HNO_3 to 100 mL. The resulting samples were measured for REE content using ICP-OES after appropriate dilution using 1% HNO_3.

2.4. Dynamic light scattering (DLS) studies

In the theory of DLS, the constant Brownian motion of suspended particles and their collision with surrounding liquid molecules is the basis of measurement; as the movent is dependent on the size of the particles. Therefore, scattered photons exposed to the moving particles can carry information about their size and can be measured as the fluctuations quantified by a correlation function. With the assumption of the spherical shape of the particles, the Stokes–Einstein equation is used to calculate hydrodynamic radius or aggregate size. Usually, it is calibrated with standards of known particle sizes [55]. The DLS studies were performed using a Malvern Nanoseries Zetasizer. The system was standardised using certified Latex standards. The temperature range of T = 50–75 °C with a temperature gradient of two degrees and one minute equilibration time was used to observe the aggregate sizes in solutions. The solution conditions are given in Table 2. For the DLS experiments, the particle size was based on size average or micellar diameter. Each measurement was performed in triplicate, and the size average was calculated for each data point by the instrument software.

3. Experimental

3.1. Solution system used in the CPE method

The aqueous solution system used in this work contained a constant ionic strength for the salts and the surfactants tested. In the literature, counter anions such as nitrate, chloride, sulphate, or, oxalate were used in the solution to maintain the pH and ionic strength [44]. Here, sodium acetate (NaOAc) and sodium nitrate ($NaNO_3$) were tested for these purposes. As the non-ionic surfactant, we used Polyethylene glycol *p*-(1,1,3,3-tetramethylbutyl)-phenyl ether, also known as Triton X-100, or

Table 1
Buffer solutions and pH range used (total volume 10 mL; surfactant: 2% v/v).

pH	Acid (mL)	Salt (mL)	Milli-Q (mL)	Surfactant (mL)
1	0.2 M HCl (4.75)	0.2 M KCl (2.45)	2.60	TX100 (0.2)
1.5	0.2 M HCl (1.63)	0.2 M KCl (2.45)	5.72	TX100 (0.2)
2	0.2 M HCl (0.52)	0.2 M KCl (2.45)	6.83	TX100 (0.2)
3	0.1 M Citric acid (4.56)	0.1 M Trisodium citrate (0.34)	4.90	TX100 (0.2)
4	0.1 M Citric acid (3.23)	0.1 M Trisodium citrate (1.67)	4.90	TX100 (0.2)
5	0.1 M Citric acid (2.01)	0.1 M Trisodium citrate (2.89)	4.90	TX100 (0.2)
6	0.1 M Citric acid (0.93)	0.1 M Trisodium citrate (4.07)	4.80	TX100 (0.2)

Table 2
Solution conditions compared by DLS studies for REE extraction by CPE (total sample volume: 10 mL; T-range: 50–75 °C).

Salt solution (mL)	Surfactant (mL)	Ligand [M]	RE Metal [M]
0.1 M $NaNO_3$ (9.8)	TX100 (0.2)	–	–
0.1 M $NaNO_3$ (9.8)	TX100 (0.2)	HDEHP [5×10^{-2}]	–
0.1 M $NaNO_3$ (9.8)	TX100 (0.2)	HDEHP [5×10^{-2}]	$Nd(NO_3)_3$ [1×10^{-3}]

briefly TX100, with linear formula: t-Oct-C_6H_4-$(OCH_2CH_2)_nOH$, n = 9–10. TX100 is used in household and industrial cleaning agents and has a low commercial price. The molecular structure of TX100 is shown in Fig. 1 along with five different multivalent ligands that were also tested in this study. There are reported range of surfactants such as Tween 80 and Span 80 that found application in the emulsion liquid membranes and extraction chromatography working at room temperatures. However, according to the literature, Triton-based surfactants are better extractants in CPE applications due to their physicochemical properties, such as having an explicit cloud point temperature and a critical micellar concentration [31,32,56]. Therefore, TX100 is used in the present study due to its advantage of exhibiting cloud-based separations at a well-defined temperature lying above room temperature. The additional advantage of the reagents used here is that they are neither volatile nor flammable, hence, environmentally more benign ("greener") than the organic extractants and diluents used in conventional hydrometallurgy of rare earths.

3.2. Optimisation of the cloud formation behaviour in the solution

CPE is a cost-effective and simple method to separate and pre-concentrate different metal ions. It has high matrix tolerance and very less environmental impact as compared to conventional hydrometallurgy. It is the reversible phase transformation phenomenon in the solution that depends on temperature change. The phase change or cloud formation takes place at a characteristic temperature, a.k.a. cloud point temperature (CPT). The cloud formation is influenced by different solution parameters, such as the surfactant. Here, the effect of the surfactant TX100 on the phase change was studied. Hereto, alkali salt and surfactant solution (10 mL) in an acid-pretreated tube were equilibrated at the start at a constant temperature of T = 20 °C with the shaker bath for 10 min. The bath temperature was then increased by 2 °C/min, followed by another 10-minute equilibration time and a visual inspection of the sample tubes for a cloud phase after that, and so forth. The experiment was discontinued at T = 80 °C.

The solution chemistry of cloud formation was also studied by changing the solution acidity, ionic strength, surfactant, and the REE-selective extractant ligand type, one at a time, by:

Acidity variation: The effect of acidity on the CPT values was studied for pH values in the range of 1 to 6 using buffer solutions with 2% (v/v) of TX100 shown in Table 1 (Section 2.2).

Ionic strength variation: Constant ionic strength in our solution was maintained using non-toxic salts, i.e., sodium acetate (NaOAc) and sodium nitrate ($NaNO_3$). Recent literature suggested the use of perchlorate media in CPE systems [44,57,58]. We avoided using such reagents to install less oxidising conditions. In addition, their use in large-scale operations would present several safety challenges due to their oxidising and pyrophoric nature.

Different ligands: Multivalent ligands are necessary for a better complexation of the REE cations to take (extract) them to a non-aqueous cloud phase. Different ligands, such as Tributyl phosphate (TBP), Bis-(2-ethylhexyl)hydrogen phosphate (HDEHP), Thenoyltrifluoroacetone (TTA), *N,N'*-dimethyl-*N,N'*-dicyclohexyl malonamide (DCMA), and, N-Methyl-*N,N,N*-trioctyl-ammonium chloride (Aliquat 336 or Al336 in brief) were used to test and to optimise the formation and extraction capabilities of the CPE (Fig. 1).

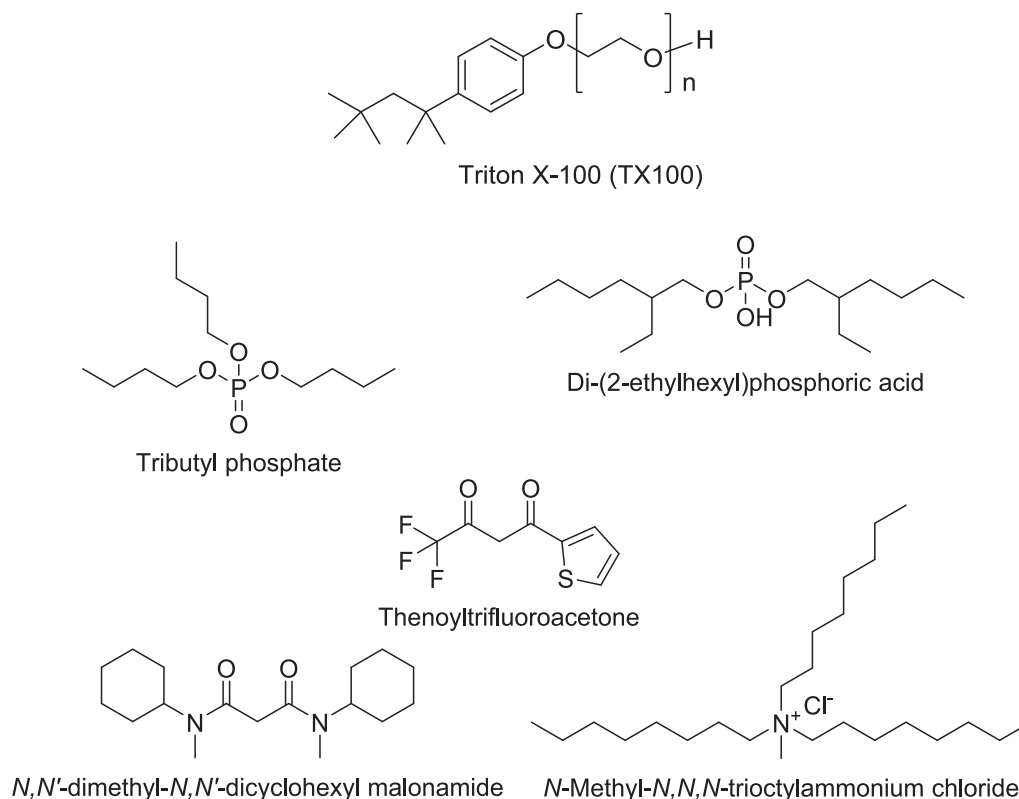More than 200 optimisation experiments were performed with

Fig. 1. Non-ionic surfactant TX100 and five multivalent ligands tested in this study.

variable acidity, ionic strength, and ligand type; before adopting the most promising experimental working conditions in further trials.

3.3. Screening of ligands for distribution of REEs

The optimised acidity and ionic strength conditions were then adopted to study the distribution of REEs from pure REE salts (in our CPE system as follows: REE salts of Nd and Dy and that of Ce in the nitrate forms were each mixed with specifically tested ligands, 0.1 M NaNO$_3$ solution, and 0.2 mL of surfactant (2% v/v) in pretreated 15 mL polypropylene tubes to avoid adsorption of metal ions by the tube wall. The tubes were sealed with Teflon tape and homogenised using a vortex homogeniser (Heidolph Reax 2000). They were heated after that in a constant temperature shaker bath as outlined at the start of Section 2.2. The CPE system under study involved testing specific ligands with concentrations varying between 5×10^{-2}–1×10^{-4} M and pure REE salts between 1×10^{-3}–1×10^{-6} M.

Ligand variation samples were shaken in the constant temperature shaker bath (60 RPM) at T = 80 °C for one hour to ensure that the cloud phase was established throughout each sample. Hettich Universal 1200 equipment was used to centrifuge the samples to achieve the two distinct phases. 100 μL of the upper phase (aqueous phase) of each tube was pipetted into a fresh pretreated 15 mL tube. The samples were diluted using 1% HNO$_3$. The slightly acidic conditions were needed to avoid hydrolysis of the REEs at higher pH values [39]. Elemental content analyses were made using ICP-OES.

The mechanism of cloud formation was investigated by using ICP-OES for element analyses and dynamic light scattering (DLS) for monitoring the size changes with the micelles in the aqueous phase before and during the CP formation with selected experimental runs at temperatures between T = 50 °C and T = 75 °C.

3.4. Data treatment

With the established CPE ("clouding") conditions, the extraction efficiency of a specific element, E(%), was calculated using equation (1).

$$E(\%) = \frac{C_t V_t - C_a V_a}{C_t V_t} \cdot 100\% \tag{1}$$

where

C_t denotes the total concentration of an element in the initial solution.
C_a the concentration of an element in the aqueous phase after phase separation.
V_t: initial total volume (10 mL).
V_a: aqueous volume after CPE (9.5 mL).
V_c: cloud phase volume (0.5 mL as determined by separating the cloud phase (CP) and measuring its volume separately for each experiment independently).

The distribution ratio, D, is defined as the ratio of the amount of a specific element extracted in the nonpolar (cloud) phase to that in the remaining aqueous phase. It was calculated as:

$$D = \frac{C_c}{C_a} = \frac{C_t(V_c + V_a) - C_a V_a}{C_a V_c} \tag{2}$$

where C_c denotes the concentration of an element in the cloud phase after phase separation, and with C_t; C_a; V_t; V_a; V_c as defined in equation (1).

Equation (3) was used to determine the stoichiometry number, x, of the HDEHP ligand (HL) with the targeted elements (Ce, Nd, Dy) in the cloud phase. Eqs. (1)–(3) were also used for the CPE data with the REEs from real HDD magnet e-waste.

$$REE^{3+}_{(Aq)} + x\, HL_{(Aq)} \rightleftarrows \left([REE \cdot L_x]\right)^{(3-x)+}_{(cloud)} + xH^+_{(Aq)} \tag{3}$$
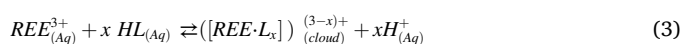
The selectivity of two different cations in the CP was calculated using equation (4).

$$S_{M1^{3+}/M2^{3+}} = \frac{D_{M1^{3+}}}{D_{M2^{3+}}} \tag{4}$$

where

S denotes the separation factor of the two metals in CPE.
$M1^{3+}$ and $M2^{3+}$: different trivalent metal ion types,
D_{M1}^{3+} and D_{M2}^{3+}: D of the respective metal types in the cloud phase after the phase separation calculated using equation (2).

3.5. Application of the optimised CPE system for Ce, Dy and Nd distribution

Nitrate forms of Nd, Ce, and Dy were each tested for their distribution under optimised CPE conditions (2)% (v/v) TX100 in 0.1 M NaNO$_3$ as a function of the HDEHP ligand concentration. Although Ce is not present in the HDD magnets, it was included here to see how a lighter lanthanide element performs under the presently applied CPE conditions.

3.6. Recycling of NdFeB-magnets from HDDs

Manual dismantling of this magnet component from the end-of-life HDD and further processing steps are indicated in Fig. 2. The demagnetisation was achieved by roasting the magnets above the Curie temperature, i.e., at T = 950 °C under 200 mL/min oxygen purging for 18 h [40]. The demagnetised piece of the NdFeB magnet was then ball-milled to a fine powder using a Fritsch Pulverisette grinding machine to serve as starting feedstock for the hydrometallurgical operations.

3.6.1. Magnet powder sample content

Magnet powder samples of about 25 mg each were mixed with 10 mL HNO$_3$, or 10 mL HCl, and 5 mL Milli-Q water before digestion in a high-pressure microwave unit (Multiwave 3000, Anton Paar, Austria), using a power of 800 W and a duration of 60 min. Each sample was then diluted in 1% HNO$_3$ to 100 mL (or more when too concentrated) for analyses of the metal ion contents by using ICP-OES.

3.6.2. Dissolution and extraction of REEs from magnet powder

After knowing the magnet elemental composition from ICP-OES, the recycling process was developed as follows: Dilute nitric acid or hydrochloric acid was added for dissolution of the fine magnet powder along with 0.1 M NaNO$_3$ and 2% (v/v) TX100. Also, powders in the absence of surfactant and salt were tested for their dissolution behaviour. The different dissolution compositions and solution conditions tested in this work are shown in Table 3.

The dissolution speed was slow due to the hardness of the NdFeB alloy in the magnet. During the magnet powder dissolution, the

Table 3
Magnet dissolution in duplicate samples (The pH value adjustment was made using the stated acids; total sample volume: 10 mL; dissolution was performed at room temperature; the dissolution and acidity patterns were observed for 14 days).

Sample Nr.	1	2	3	4	5	6
Magnet powder	25 ± 0.3 mg per tube					
9.8 mL salt solution	Milli-Q	0.1 M NaNO$_3$	0.1 M NaNO$_3$	0.1 M NaNO$_3$	0.1 M NaNO$_3$	–
+ acid solution	–	–	pH = 2 HCl	pH = 2 HNO$_3$	pH = 1 HNO$_3$	1% HNO$_3$
+ 0.2 mL surfactant	TX100	TX100	TX100	TX100	TX100	–

supernatant solution was sampled in regular time intervals (24 h), centrifuged, and its dissolved metal contents were determined using ICP-OES. After 14 days, the remaining undissolved magnet powder was separated from the liquid phase by centrifugation, dried in a furnace, and weighed at room temperature. The supernatant solution was heated at T = 80 °C for 1 h to separate the REEs from other impurities (such as transition metals) co-present with the HDD magnet using CPE. After each CPE experiment with the dissolved magnet powder constituents (Table 3), the amounts of REEs remaining in the aqueous phase were determined by ICP-OES, and the values were subtracted numerically from the amount of REEs found in the control samples (i.e. taken before the extraction experiment) to calculate the amount residing in the cloud phase. The selectivity of two different metal cations in the cloud phase was then calculated using equation (4) (Section 3.4).

Lastly, oxalic acid was added in a stoichiometric amount to the cloud phase to precipitate all of the REEs. The remaining layer of surfactant and ligand was then recycled back to the CPE system (Fig. 3), along with the aqueous phase-containing NaNO$_3$, making the overall process green. The respective oxide form of the REEs recycled from the magnet waste was obtained after calcination of the oxalates at T = 950 °C, because this would be an economically acceptable product of the recycling process, as well as, a good starting point for transferring it upon customer request in other salt forms, such as nitrates for instance.

4. Results and discussion

4.1. Optimisation of CPE solution system

Surfactant TX100 showed a distinct CPT at different solution conditions (Section 3.2). The different phases in the cloud formation process are shown in Fig. 4: "clear homogeneous", "turbid homogeneous", "bubbles forming" and "two distinct phases" that are usually seen when heating the CPE system to T = 80 °C.

Further optimisation of the CPE solution system included varying the acidity and the ionic strength. At different experimental conditions, the variation of each parameter had a discernible effect on the CPT.
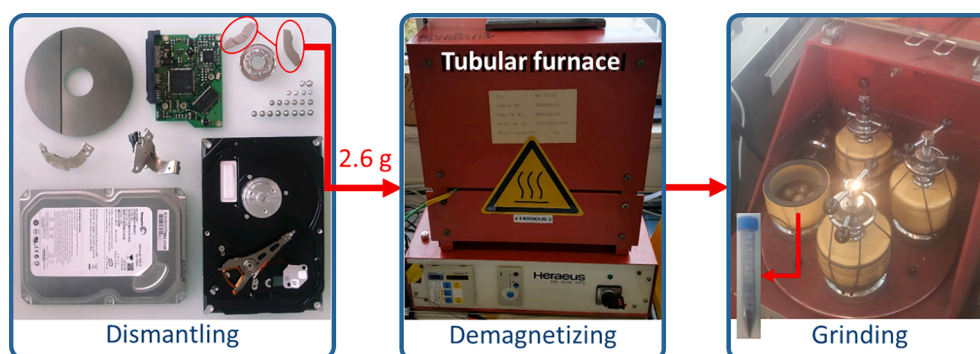

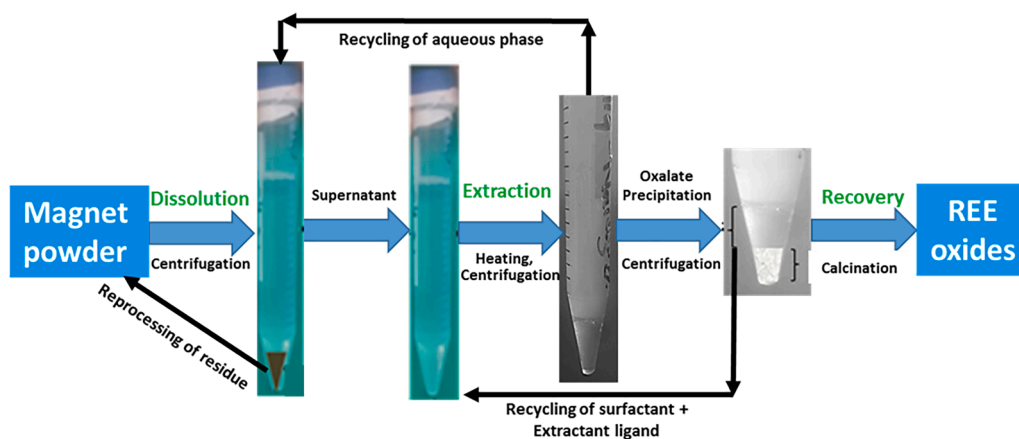**Fig. 2.** Mechanical and physical processing of HDD e-waste.

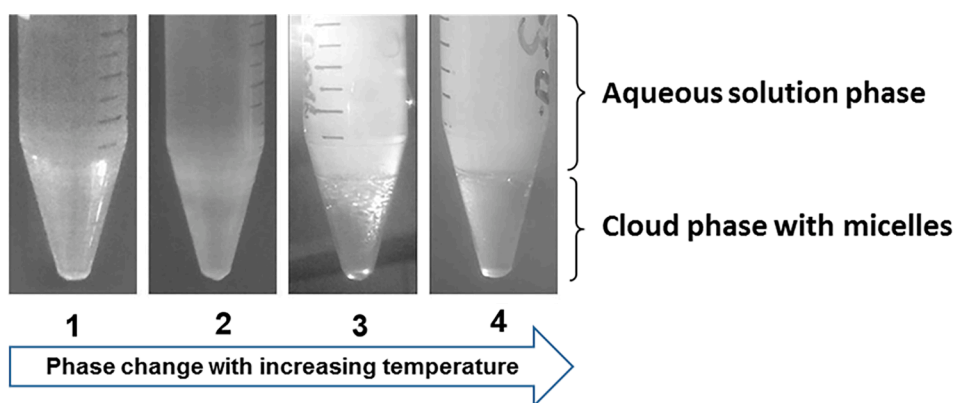**Fig. 3.** Key steps in the developed CPE process.

Fig. 4. Cloud formation with 2% v/v aqueous solution of TX100 between T = 20–80 °C (Phases: 1. "clear" solution, 2. turbid, 3. bubbles, 4. two distinct phases).

Different buffer systems (Table 1) were used to determine the CPT at several pH values between pH = 1 and pH = 6. From Fig. 5, it was found that the CPT value decreases gradually with increasing pH value from T = 74 °C for pH = 1 to T = 68 °C for pH = 5.6.

Ionic strength: The effect of ionic strength variation on the TX100-based CPE system can be compared with the model literature system of

Triton X-114 (or briefly TX114). TX114 stands for (1,1,3,3-Tetramethylbutyl)phenyl-polyethylene glycol, Polyethylene glycol *tert*-octylphenyl ether; linear formula: $(C_2H_4O)_n\ C_{14}H_{22}O$, n = 7 or 8). The CPT and the pH values with the TX100 system in the presence of different alkali salts ($NaNO_3$, NaOAc), but without a ligand, were determined as a function of the ionic strength from added salt ($NaNO_3$, NaOAc) with [Salt] = 0.01–0.10 M (Fig. 6). Those with the ligand TX114 with the same salts and in presence of a ligand were reported by Kumari et al. [44].

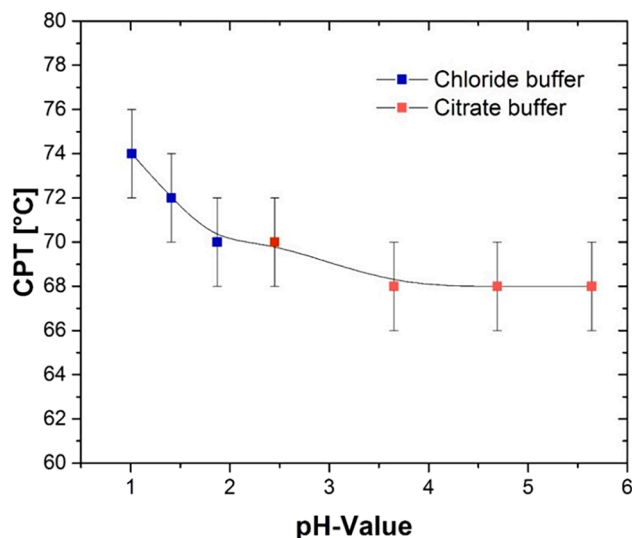Both surfactants showed quite stable CPT courses. Changing less than

Fig. 5. Effect of pH value on CPT of TX100. (Surfactant: TX100 (2% v/v); Solution medium: Chloride buffer solutions for pH = 2 and citrate buffer solutions for pH = 3–6; Total solution volume: 10 mL).
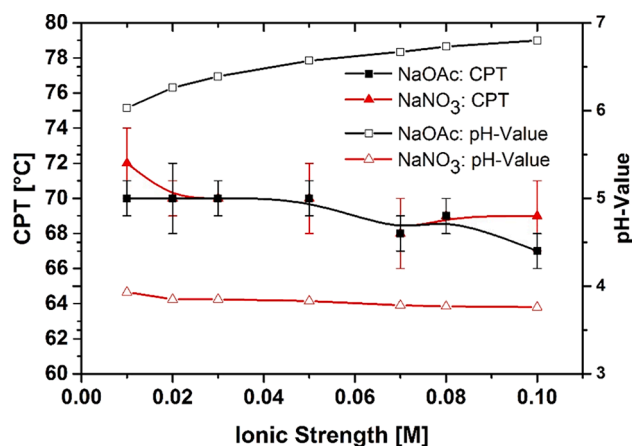

Fig. 6. Effect of ionic strength of alkali salts ($NaNO_3$, NaOAc) on the CPT and the pH value with the surfactant TX100 (2% v/v) CPE system.
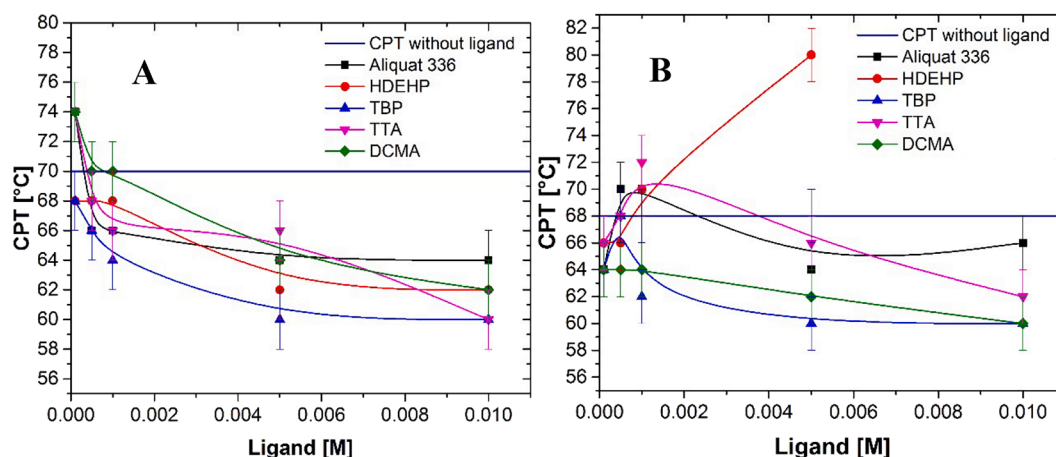
Fig. 7. Effect of ligand concentration on CPT of TX100. (Surfactant: TX100 (2% v/v); **A**: 0.1 M NaNO$_3$ medium; **B**: 0.1 M NaOAc medium; Horizontal line indicates the control condition, i.e., the CPT without ligand).

2–3 °C in the course of the ionic strength variations, but with markedly different CPT values. This is due to the high solubility of TX114, rendering CPT values at room temperature (T = 23 °C) [44,57]. As for the pH, TX114 exhibited pH values increasing from 5 to 6 with increasing NaNO$_3$ ionic strength and from 7 to 8 with NaOAc. TX114 pH also showed pH values increasing from 6 to 7 with increasing NaOAc, but nearly constant pH values with NaNO$_3$. Given the above, the nearly neutral acidity and the tailorable CPT range at temperatures lying clearly above room temperature promise better control of the extraction process with TX100. Therefore, it was the surfactant of choice in this study.

Ligand type: The ligand type variation was performed with 2% (v/v) TX100 under three different solution conditions, i.e., in only deionised (Milli-Q) water, in 0.1 M NaOAc, or in 0.1 M NaNO$_3$. In Milli-Q water, the CPT using the ligand HDEHP was found at T = 82 °C. It was determined to rule out any impact from ionic strength or buffer solution. In total, five ligands (Section 3.2) were employed to determine the CPT as a function of their concentration in an aqueous 0.1 M NaNO$_3$ medium and with TX100 as the surfactant (Fig. 7A). The ligand concentration variation experiment was also carried out with TX100 in an aqueous 0.1 M NaOAc medium (Fig. 7B). Without ligand, the CPT value of T = 70 °C with TX100 in the NaNO$_3$ medium and that of T = 68 °C in the NaOAc medium lies close to earlier cited CPT values for TX100 with monovalent alkali salts of about T = 65 °C-67 °C [44,46].

In the 0.1 M NaNO$_3$ medium (Fig. 7A), the CPT with the ligands TBP and HDEHP at the lowest concentration studied (0.0001 M) was 2 °C lower than the value of T = 70 °C measured without a ligand ("control condition"). However, for DCMA, TTA, and Aliquat 336 ("Al336"), the CPT was 4 °C higher. Each ligand showed inverse trends for the CPT with increasing ligand concentration. At the highest ligand concentration studied (0.01 M), all CPT values laid 4–6 °C below the "control condition" result (T = 70 °C). In the 0.1 M NaOAc medium (Fig. 7B), initially increasing CPT trends were observed with all ligand types. Except with HDEHP, all other ligands then more or less passed through a maximum around or below 0.001 M, before decreasing after that towards CPT values laying well below that of the "control condition" (T = 68 °C). With [HDEHP] = 0.01 M, the CPT may well lie above the temperature limit of the heating bath (T = 95 °C with a LAUDA E200 thermostat) and could therefore not be determined.

From the above, we choose to use a constant ionic strength of 0.1 M NaNO$_3$ as the solution condition for subsequent experiments that are presented in the next section. Moreover, nitrate is also the form with most of the purchasable REE salts, along with the chloride, sulphate, oxide and oxalate forms.
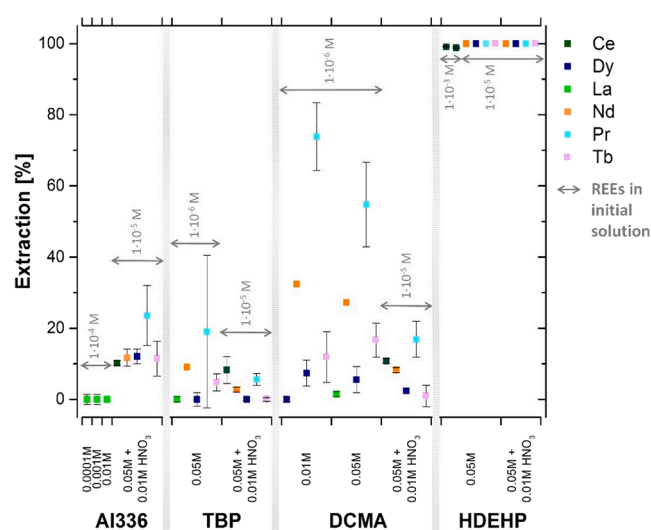

Fig. 8. Extraction efficiency of different ligands using CPE. (Surfactant: TX-100 (2% v/v); medium: 0.1 M NaNO$_3$; [REE]: $1 \times 10^{-3} - 1 \times 10^{-6}$M; indicated with the horizontal double-arrowed bars).

4.2. Performance of the selected extractant ligands

Due to the decrease of the CPT with the NaNO$_3$ medium with increasing ligand concentration (Fig. 7A), four ligands (Al336, TBP, DCMA, HDEHP) were also tested in NaNO$_3$ medium for extracting specific REEs (Dy, La, Nd, Pr, Tb) and Ce in their cloud phases (Fig. 8). Dy, La, Nd, and Ce extractions were performed in the pure nitrate form; Pr and Tb were part of the multi-REE solution used for the calibration of the ICP-OES (Section 2.1).

Al336 and TBP showed overall poor extraction performances, irrespective of the presence, or, absence of acid. DCMA only showed a good extraction performance for praseodymium (Pr), but it dropped substantially when HNO$_3$ was also added to the system. With lower extraction performance, the ICP-OES data accuracy was also poorer. In contrast, the extraction performance with 0.05 M HDEHP was very well. Single REE concentrations of 1x10^{-3}M in the absence of acid revealed near-quantitative extraction efficiencies (E > 95%), but with 1x10^{-5} M single REE feeds and dilute acid practically quantitative extraction efficiencies were obtained (E > 99%).

The poor extraction performances of Al336, TBP, and DCMA could be attributed to their less lipophilic nature when compared to the HDEHP ligand. The presence of two ethylhexyl alkyl sidechains with
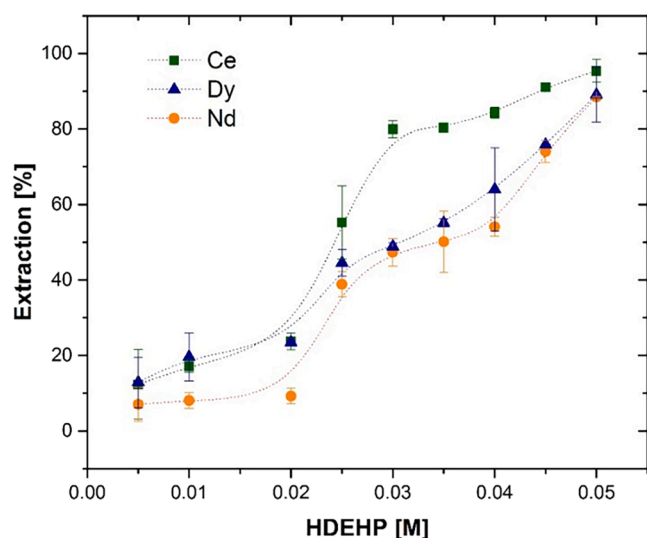
Fig. 9. Extraction (in %) for REEs using CPE under varying ligand concentration of HDEHP (Surfactant: TX100 (2% v/v); medium: 0.1 M NaNO$_3$; [single REE feed solution]: 1×10^{-3}M; [HDEHP]: 5×10^{-3}-5×10^{-2} M).

HDEHP renders it more lipophilic, hence, promotes the transfer of the metal–ligand complex to the cloud phase due to its poorer solubility in the aqueous phase. In addition, the efficiency of the CPE also seems to be underlined by the fact that it required substantially less HDEHP inventory and the extraction was also excellent even in the absence of organic diluent. This is advantageous in terms of efficiency as well as environmental impact when compared to conventional hydrometallurgy means [46–49]. Summarising the above, out of the five different multivalent ligands studied in the developed CPE system, 0.05 M HDEHP and 2% (v/v) TX100 in 0.1 M NaNO$_3$ medium performed by far the best and it was therefore selected for further testing with a metal feed solution prepared from real NdFeB magnets. These and other results are presented further down the text in Section 4.

Fig. 9 shows the extraction efficiencies (calculated with equation (1)) of the CPE system for Ce, Dy, and Nd, as a function of the HDEHP ligand concentration in the presence of a constant concentrated TX100

(surfactant) and NaNO$_3$ medium, using differently concentrated single cationic element feed runs. At the highest ligand concentration ([HDEHP] = 0.05 M), the highest extraction efficiencies were achieved, i.e., E = 95.4%, 89.1%, and 88.4% for Ce, Dy, and Nd, respectively. Using the experimental CPE results from the single REE feeds, equation (2) was used to calculate the distribution ratio, D, for three elements (Nd, Dy, Ce) determined in the cloud and the aqueous phase resulting after clouding, as a function of the HDEHP ligand concentration. The logarithmic values of D over the same [HDEHP] range on a logarithmic scale are shown in Fig. 10A; those in the red-bordered section with Fig. 10A are shown enlarged in Fig. 10B.

The overall-calculated slope with the data in this logarithmic plot is equivalent to the number of ligands involved in the complex (equation (3)), i.e., the regression for Nd showed the involvement of more than one complex species in the high range of HDEHP concentrations studied. Generalising the results for elevated HDEHP concentrations $\geq 2.5 \times 10^{-2}$ M (thus for log[HDEHP] $\geq$ -1.6), the three calculated slope values (Fig. 10B) suggest that typically three HDEHP ligands are coordinating with each trivalent cation studied (Ce^{3+}, Dy^{3+}, Nd^{3+}). At lower HDEHP concentrations, the log D values (Fig. 10A) changed hardly for Nd, and only slightly for Ce and Dy with calculated slopes $\sim$ 0.6. The initial trend suggest the prerequisite of a critical minimum HDEHP concentration with the present CPE system. Both findings are at least also in line with other reported general complexation behaviour of HDEHP in a molecular diluent medium as expressed by equation (3) and here with a stoichiometric number x≈2.4–3.6 [14,16].

The extraction efficiency of the conventional solvent extraction methods is close to 90% but with at least ten times higher ligand concentration as compared to our proposed approach [15,16,59]. The CPE method has also a clear advantage regarding the stripping difficulties of the HDEHP ligand because after the temperature change the cloud formation is reversible. Therefore, after the separation of the remaining aqueous medium and getting the cloud solution at room temperature, the lipophilicity of the cloud phase is lost, and in such conditions, the binding of metals with HDEHP is not possible due to the non-homogeneity of the solution. In such conditions, the metals are free from the ligand and can be separated easily using oxalate precipitation. Therefore, there is no apparent stripping issue in our developed extraction system. An efficiency close to 10–15% had been reported for light REEs in the literature [59]. In comparison to the presently studied
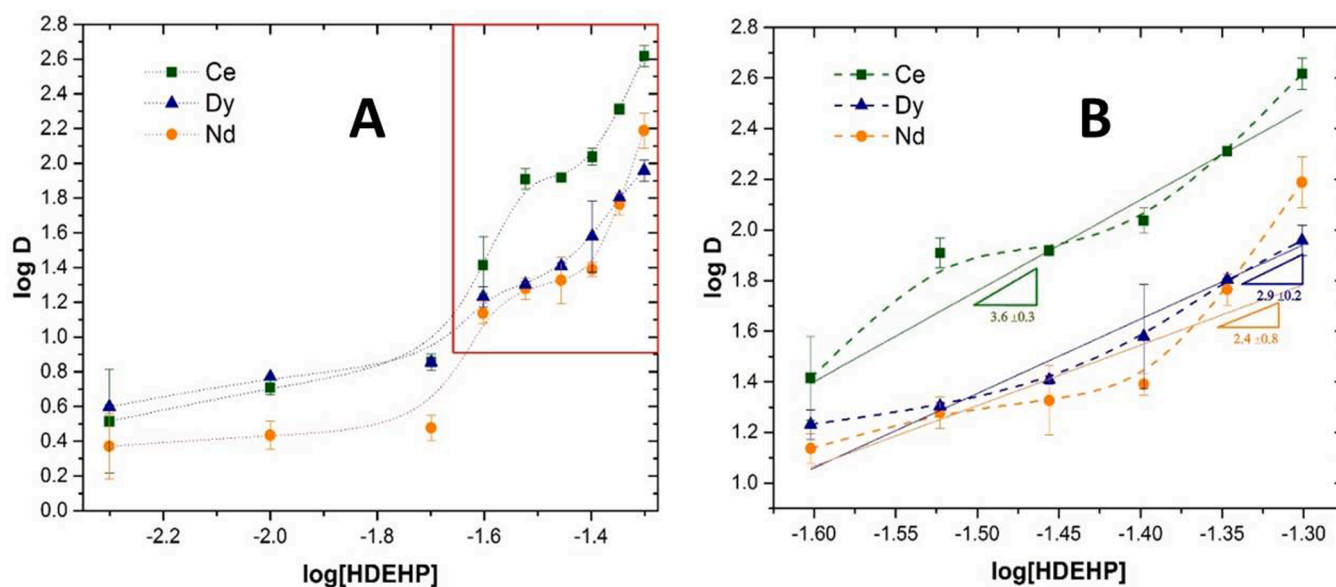
Fig. 10. **A:** Logarithmic values of the distribution ratio D for Ce, Dy, and Nd, as a function of the log value of the HDEHP concentration. (Surfactant: TX100 (2% v/v); medium: 0.1 M NaNO$_3$; [REE] in feed solution: 1×10^{-3}M; [HDEHP]: 5×10^{-3}-5×10^{-2} M). **B:** Enlargement of the red-bordered rectangle shown in Fig. 10A, together with complexation stoichiometry numbers derived from the slopes of the lines drawn through each data set.

Fig. 11. Aggregate size of micelles from DLS experiments as a function of the temperature in CPE runs with selected solutions (Table 2). Surfactant: TX100 (2% v/v).
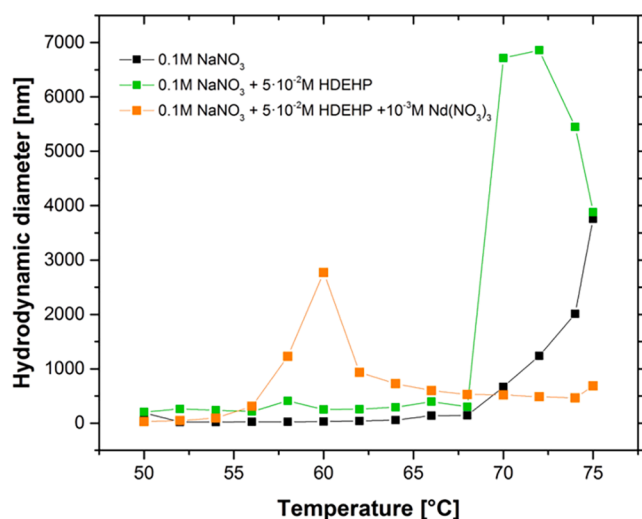
cloud point extraction method which showed impressive efficiencies of nearly 95% for La and Gd even in a neutral pH medium. Therefore our process gives the advantage to work with less ligand inventory and at an acid strength slightly less than pH = 1 to have higher loading capacities to process REEs purification without hydrolysing or precipitating them.

4.3. DLS studies of the CPE in the presence of HDEHP ligand

DLS measurements were performed to track any changes in the solution, such as the micelles in the pristine solution, size growth, and the collapse of micelles into aggregates with the cloud phase. For the DLS experiments, the particle size based on size average or micellar diameter was used. The different solution conditions in this DLS study are shown in Table 2 (Section 2.4). The average hydrodynamic diameter of such entities as a function of the temperature and the abrupt increase of micelle size at the CPT are shown in Fig. 11.

The DLS measurements with 0.1 M NaNO$_3$ medium revealed that the control system (i.e. surfactant without ligand), as well as, the system with 2% (v/v) TX100 as a surfactant and 0.05 M HDEHP as ligand both showed their onset to micellar aggregate formation at about T = 68 °C (Fig. 11). However, when the last-mentioned system included soluble Nd nitrate, the onset started at much lower temperatures (T = 56 °C). The drop in CPT is also reported for other systems in the literature, and it is attributed to the added salt in that its cations may remove water molecules from the micelles at lower temperatures due to the coordinate bonding effect and the formation of an overall lipophilic system with the ligand molecules and the added cations into one complex moiety [39]. Therefore, and in agreement with our visual observations, it may be concluded here that at the CPT, the micelles had collapsed (aggregated) into a lipophilic cloud. This result cannot be compared with the optimisation trials presented in Section 2.2 involving the use of the constant-temperature-shaking bath due to the absence of the possibility of stirring and much shorter equilibration time with the DLS measurements. Notwithstanding these, the DLS results support the mechanism of increasing micellar sizes and their collapse due to aggregation at the CPT. Moreover, in the presence of trivalent REE cations from added salt (Nd(NO$_3$)$_3$), an additional effect of lipophilic metal–ligand complexation is observed.

4.4. CPE mechanism

Based on the CP and the DLS results in this study, the CPE mechanism for rare earth and other trivalent cations and in particular with the HDEHP ligand can be understood and visualised (Fig. 12) as follows: Initially, all the CP solution ingredients are mixed. Based on the HSAB theory [39] and the cation exchange mechanism, the REEs behave as hard acids to bind with the hard-base ligand HDEHP by exchanging acidic protons (equation (3). The equilibration occurs in the solution. The HDEHP ligand has lipophilic alkyl side chains outside the metal–ligand complex (Fig. 1) that can form aggregates with the TX100 surfactant. With the increase in temperature, the micellar size increases due to the increased lipophilicity of the surfactant molecules. At the CPT, the lipophilic metal–ligand complexes become highly hydrophobic and collapse to form the cloud phase at the bottom of the tube due to their lipophilic nature. Compared to the other ligands studied here (Fig. 1),
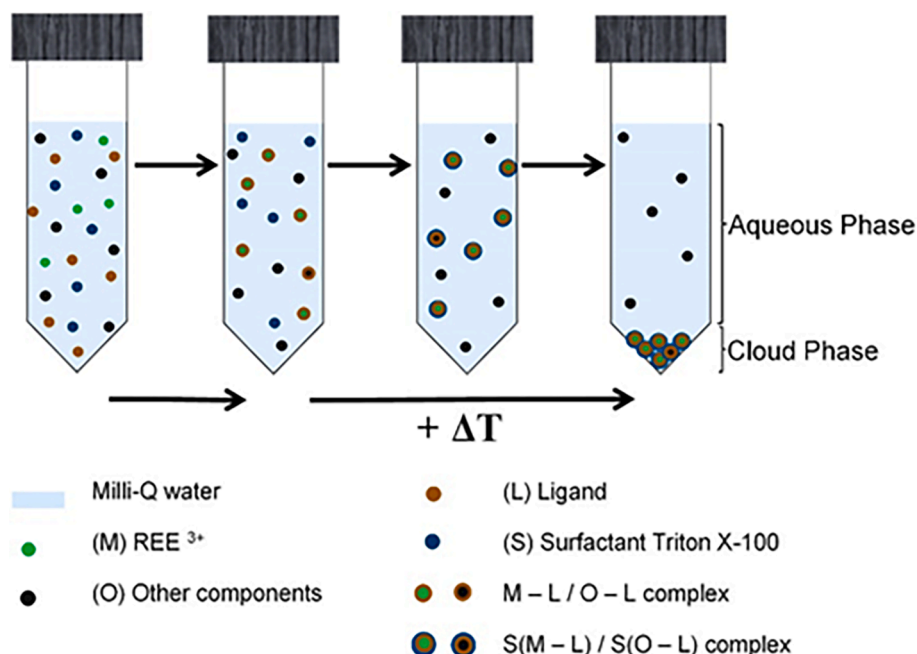

Fig. 12. Plausible mechanism for REE-ligand-surfactant rich phase formation in the studied CPE conditions (Surfactant: TX100).

Table 4

Characterisation of the NdFeB e-waste magnets used in this study. The average and standard deviation values were calculated from the analysis of three magnet samples.

Composition of HDD magnet used in the present work (element Wt.-%)	
Nd	21.3 ± 0.2
Dy	1.40 ± 0.02
Pr	4.7 ± 0.1
Sm	0.57 ± 0.01
Er	0.23 ± 0.02
Co	0.42 ± 0.01
Fe	59.3 ± 0.4
Ni	7.0 ± 0.1
B	0.99 ± 0.01
Mg	1.3 ± 0.3
Si	0.6 ± 0.2
Al	0.7 ± 0.1
Total	**98.5**[#]

[#] The deviation from 100 wt-% is due to the co-presence of other metal traces not considered in the present calculations.

HDEHP showed the best extraction behaviour due to the 16 carbon molecules in its structure raising the lipophilic nature of the metal–ligand complex. The cloud phase was observed at somewhat higher temperatures with higher concentrated acid concentrations (Fig. 5), likely because the presence of additional H^+ binds to the surfactant's oxygen atom through hydrogen bonding, thus, keeping it polar for a prolonged duration at higher temperatures. However, the opposite effect is observed when varying the ionic strength within the system, because a higher ionic strength helps to take water molecules away from the micelles so that the micelles can form a cloud phase at somewhat lower temperatures.

5. Process development for REE extraction from HDDs

The best performing CPE system with 0.05 M HDEHP ligand, 2% (v/v) TX100 surfactant in 0.1 M NaNO$_3$ medium was applied to the feed solution prepared from real NdFeB magnets. The elemental composition of the "NdFeB" magnet is that of the $Nd_2Fe_{14}B$ alloy. From the ICP-OES results (Table 4), it was inferred that the Fe/Nd Wt.-% ratio equalled 2.78 ± 0.01, thus, in agreement with the literature [40].

The values are comparable to the composition reported in the literature. The somewhat higher amounts of Ni, Pr, and Al can be attributed to different manufacturers, as well as, to a slightly different chemical configuration of the magnets used in the present work. The specific composition of the magnets can vary depending on the manufacturer, year of production, and intended use. The overall mechanical and digestion process for recycling is the same; irrespective of the composition of the NdFeB magnets. However, the solution chemistry may need further optimisation depending on the metal composition of the magnets used for recycling, their origin, and the presence of other waste contaminants.

The CPE method was applied to the demagnetised magnet powder after its dissolution in acid (Section 3.6.2). The acidity was neutralised within the digestion process. The solution was then used for subsequent CPE directly after having added the surfactant. In some experiments, the dissolution of the demagnetised magnet powder was done by adding the surfactant and nitrate salt at the forehand. The solution compositions are shown in Table 3 (Section 3.6.2). In the absence of acid (i.e. in deionised Milli-Q water or 0.1 M NaNO$_3$ solution), a very small dissolution was observed (Fig. 13A).

The highest dissolution was observed either in 1% HNO$_3$ or in 0.1 M HNO$_3$ (pH = 1) solutions. The suitable solution media that can also fulfil the condition of the neutralisation of the acid during the dissolution was found to be with 0.01 M HNO$_3$ (pH = 2), and it afforded an effective dissolution as well (Fig. 13A). The remaining undissolved magnet residue can be recycled back within the process. The dissolution pattern as
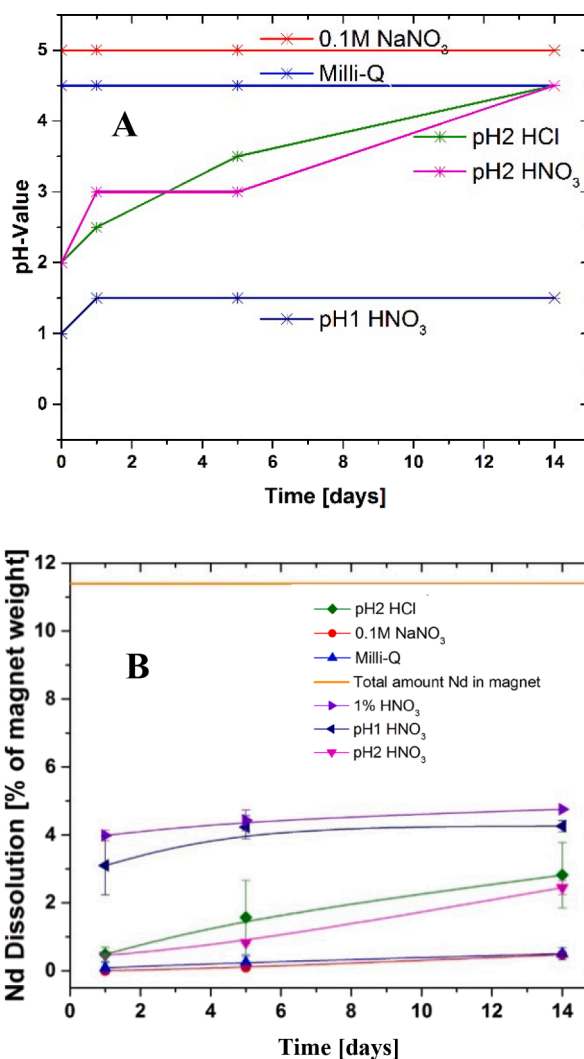

Fig. 13. Dissolution of magnet powder in different solution conditions **A:** effect on acidity with time and dissolution. **B:** the amount of dissolution based on ICP-OES measurement of the supernatant solution. (The acidities of the NaNO$_3$ and Milli-Q solutions were slightly higher due to magnet powder components).

a function of time (days) for Nd is shown in Fig. 13B; those of the other metals co-present with the NdFeB magnet (Al, B, Co, Fe, Ni, Pr, Dy) are shown in Figures A-G in the Appendix.

After the dissolution of the magnet powder, HDEHP was added to the supernatant solution to make a 0.05 M ligand concentration in the solution and then heated in a constant temperature-shaking bath. After heating, precipitation occurred due to the salting-out effect. Depending on the actual saturation levels and salting-out impact, a varying amount of precipitate was observed exhibiting white to brown, but also orange colours, depending on the acidity of the acid solution used, which was ranging from 1% HNO$_3$ to 0.1 M HNO$_3$. The precipitates formed were found to contain Nd, Dy, Pr, Al and Fe, but no B, Co, or Ni. Therefore, they were left behind with the aqueous phase and can thus be separated from the cloud phase entirely.

Fig. 14A shows that hardly any extraction of Nd^{3+} occurred in only de-ionized (Milli-Q) water. It was also found that the co-presence of NaNO$_3$ was needed to transfer the Nd^{3+} ions into the cloud phase. For Nd, quantitative extraction was observed in 0.01 M ("pH2") HCl medium, whereas the extraction performance of 98% under 0.01 M ("pH2") HNO$_3$ was also very satisfactory. Less well was the extraction result for Nd^{3+} with the 0.1 M ("pH1") HNO$_3$ medium ($\approx$45%). Fig. 14B shows the extraction efficiencies for three targeted REEs (Nd, Dy, Pr) and those of
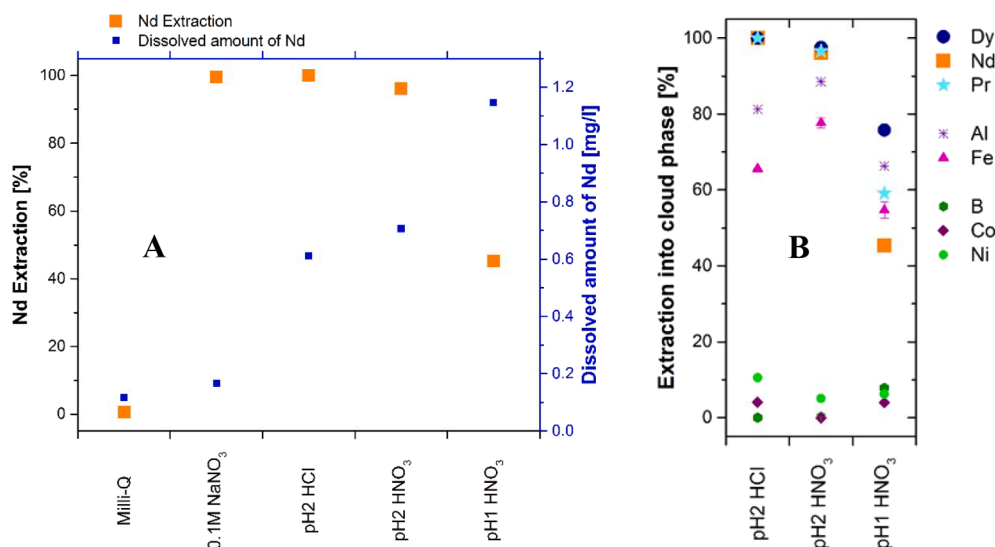
Fig. 14. Separation of REEs from dissolved magnet powder using CPE in different solution conditions. (**A:** amount of Nd dissolution and the corresponding extraction efficiency. **B:** extraction efficiency of different metals).

Table 5
Separation factor (S) for Nd, Dy, and Pr from magnet waste achieved with CPE (**M1:** metal ion for which the separation factor was calculated, **M2:** metal ion to which the M1 separation factor is to be compared with (see equation (4)).

pH = 2 HCl		M1			pH = 2 HNO$_3$		M1		
		Nd	Dy	Pr			Nd	Dy	Pr
M2	Nd	1	1.219	1.223	M2	Nd	1	1.014	1.004
	Dy	0.820	1	1.003		Dy	0.986	1	0.990
	Pr	0.818	0.997	1		Pr	0.996	1.010	1
	Al	1.005	1.226	1.229		Al	1.087	1.102	1.091
	Fe	0.824	1.004	1.007		Fe	1.033	1.048	1.038
	B	2051	2501	2508		B	376	381	378
	Co	19.9	24.3	24.4		Co	839	850	842
	Ni	7.75	9.45	9.47		Ni	19.06	19.33	19.14

other elements (Al, Fe, B, Co, Ni) co-present with the NdFeB magnet e-waste. All of the three targeted REEs (Nd, Dy, Pr) showed quantitative extraction performance with the 0.01 M ("pH2") HCl medium, near-quantitative performance with the 0.01 M ("pH2") HNO$_3$ with 98%, 96% and 97%, respectively, but with 0.1 M ("pH1") HNO$_3$ medium it was fair with Dy (~77%), with Pr (~60%) and with Nd (~45%).

Managing both acidities for the leaching and extraction performance is a challenge and requires contradicting conditions. Our approach has been substantially successful in managing this challenge. As shown in Fig. 14, we can manage the dissolution as well as the Nd extraction (>90%). We used the same acid medium for the extraction without neutralisation or dilution. Also after extraction, it is the merit of the CPE technique that the metal content collapses in (is restricted to) the cloud phase and that the remaining aqueous solution can be separated easily by centrifugation without loss of acid. The extraction selectivity of the trivalent ions found with the cloud phase was calculated using equation (4) and the results are shown in Table 5. These metal ions were then precipitated completely using stoichiometric oxalic acid and removed from the cloud phase after centrifugation. Therefore, the aqueous phase and the cloud-containing metal-free ligand and surfactant are available again for recycling in a new extraction loop. The REEs containing precipitate was then calcinated at T = 950 °C to give Nd, Dy and Pr as metal oxides. Such mixtures could be used directly for magnet manufacturing, or, other tailor-made applications and compositions.

For the sake of the homogeneous experiment (Fig. 2), the pulverisation (grinding) step was done for the effective dissolution of the small amounts used in this work. However, it can be avoided on a larger scale by using a direct acid digestion step (i.e. without the need for grinding or

demagnetisation as everything dissolves in solution) in the future. The amount of energy required for the actual chemical recovery process is then due to the heating of the solution for cloud formation. The energy requirement is 231 kJ per litre of the processing solution to heat the solution to T = 80 °C. One could apply energy from green energy resources to keep the impact low. It is also possible to use a higher temperature gradient to reach the CPT with the CPE solution system faster, thereby also reducing the overall processing time. Or, in technical REE recycling applications with magnet e-waste, one could consider using TX114 with its CPT around room temperature instead of TX100, provided that TX114 proves equally effective as the TX100 ligand.

The advantages of the CP method over conventional liquid–liquid extraction are undeniable as it needs much less ligand inventory and no organic diluents, it delivers concentrated separated metals in small cloud volumes that can be processed further in reduced volumes of liquid, and the CPE components are recyclable and reusable several times. The CPE product from magnet e-waste could be used for manufacturing new Nd magnets [60]. Or, it can be purified further using transition metal removal techniques.

6. Conclusions

Cloud Point Extraction (CPE) has been presented for preconcentration or enrichment tasks in the recycling of REEs from NdFeB magnet e-waste. The method was optimised for dissolution and extraction efficiency. Surfactant Triton X-100 (TX100), solution conditions such as acidity (pH = 1–6), ionic strength (0–0.1 M NaNO$_3$ or NaOAc) and several different non-ionic ligands with different concentrations

(0–0.05 M) were studied. Out of the five different extractant ligands tested, bis-(2-ethylhexyl)-phosphoric acid (HDEHP) was by far the best. The CPE mechanism was investigated using DLS and showed a clear trend for increasing micelle formations with REE-containing solutions and their collapse (aggregation) in an additionally formed cloud phase at a cloud phase temperature (CPT) at T = 56 °C and without REEs at T = 68 °C. The developed recycling method has been applied to real NdFeB magnets taken from a discarded hard disk drive to recycle key metals like Nd, Dy and Pr. The amount of ligand and other solution components required for the recycling of REEs using this CPE method is substantially less when compared with conventional hydrometallurgical approaches. The diluted acid solutions (HCl or HNO_3 at a value of pH = 2) used for the dissolution of the magnet powder were either neutralised by consumption or reused within the same CPE-based separations. With our optimised system, >95% of REEs were extracted in the cloud phase using single REE feeds. In our application with NdFeB magnet waste, also a high separation of REEs was achieved over the co-presence of non-REE impurities, such as B, Co and Ni.

The current work involved basic complexation chemistry development in a cloud medium. Moreover, the process parameters achieved with real magnet e-waste involved much less environmental impact as compared to current mining practices and metal resources value chains. Therefore, it would substantially contribute to a circular economy, urban mining and alternative resources development from the wastes. The output products are suitable for the new Nd magnet manufacturing making the circular loop of REE metals.

CRediT authorship contribution statement

Ajay B. Patil: Conceptualization, Data curation, Formal analysis, Funding acquisition, Investigation, Methodology, Project administration, Validation, Visualization, Writing – original draft, Writing – review & editing. **Nicole Thalmann:** Data curation, Formal analysis, Investigation, Validation, Visualization, Writing – original draft. **Laura Torrent:** Methodology. **Mohamed Tarik:** Data curation, Formal analysis, Validation, Writing – review & editing. **Rudolf P.W.J. Struis:** Conceptualization, Data curation, Funding acquisition, Investigation, Project administration, Supervision, Validation, Visualization, Writing – review & editing. **Christian Ludwig:** Conceptualization, Funding acquisition, Supervision, Validation, Writing – review & editing.

Declaration of Competing Interest

The authors declare that they have no known competing financial interests or personal relationships that could have appeared to influence the work reported in this paper.

Data availability

Data will be made available on request.

Acknowledgements

Appendix A. Supplementary material

Supplementary data to this article can be found online at https://doi.org/10.1016/j.molliq.2023.121905.

References

[1] C.P. Balde, V. Forti, V. Gray, R. Kuehr, P. Stegmann, The global e-waste monitor 2017, 2017. 10.1016/j.proci.2014.05.148.

[2] J. Burlakovs, Y. Jani, M. Kriipsalu, Z. Vincevica-Gaile, F. Kaczala, G. Celma, R. Ozola, L. Rozina, V. Rudovica, M. Hogland, A. Viksna, K.M. Pehme, W. Hogland, M. Klavins, On the way to 'zero waste' management: Recovery potential of elements, including rare earth elements, from fine fraction of waste, J. Clean. Prod. 186 (2018) 81–90, https://doi.org/10.1016/j.clepro.2018.03.102.

[3] B. Achzet, A. Reller, C. Rennie, M. Ashfield, J. Simmons, Materials critical to the energy industry. An introduction., in: Commun., University of Augsburg, 2011.

[4] I.F.W. Lima, Rare Earths Industry, 2016th ed., Elsevier, 2016. 10.1016/c2014-0-01863-1.

[5] S. Massari, M. Ruberti, Rare earth elements as critical raw materials: Focus on international markets and future strategies, Resour. Policy. 38 (2013) 36–43, https://doi.org/10.1016/J.RESOURPOL.2012.07.001.

[6] J.H. Rademaker, R. Kleijn, Y. Yang, Recycling as a strategy against rare earth element criticality: A systemic evaluation of the potential yield of NdFeB magnet recycling, Environ. Sci. Technol. 47 (2013) 10129–10136, https://doi.org/10.1021/es305007w.

[7] A.B. Patil, R.P.W.J. Struis, A.J. Schuler, M. Tarik, A. Krebs, W. Larsen, C. Ludwig, Rare Earth Metals Recycling from E-Wastes: Strategy and Perspective, in: C. Ludwig, S. Valdivia (Eds.), Prog. Towar. Resour. Revolut., World Resources Forum, Villligen PSI and St. Gallen, 2019: pp. 162–164.

[8] L. Ciacci, I. Vassura, Z. Cao, G. Liu, F. Passarini, Recovering the "new twin": Analysis of secondary neodymium sources and recycling potentials in Europe, Resour. Conserv. Recycl. 142 (2019) 143–152, https://doi.org/10.1016/j.resconrec.2018.11.024.

[9] M. Moore, A. Gebert, M. Stoica, M. Uhlemann, W. Löser, A route for recycling Nd from Nd-Fe-B magnets using Cu melts, J. Alloys Compd. 647 (2015) 997–1006, https://doi.org/10.1016/j.jallcom.2015.05.238.

[10] A.B. Patil, M. Tarik, R.P.W.J. Struis, C. Ludwig, Exploiting end-of-life lamps fluorescent powder e-waste as a secondary resource for critical rare earth metals, Resour. Conserv. Recycl. 164 (2021), 105153, https://doi.org/10.1016/j.resconrec.2020.105153.

[11] K. Binnemans, P.T. Jones, B. Blanpain, T. Van Gerven, Y. Yang, A. Walton, M. Buchert, Recycling of rare earths: A critical review, J. Clean. Prod. 51 (2013) 1–22, https://doi.org/10.1016/j.jclepro.2012.12.037.

[12] R. Kumar, T. Thenepalli, J. Whan, P. Kumar, K. Woo, J. Lee, Review of rare earth elements recovery from secondary resources for clean energy technologies: Grand opportunities to create wealth from waste, J. Clean. Prod. 267 (2020), 122048, https://doi.org/10.1016/j.jclepro.2020.122048.

[13] K.M. Goodenough, J. Schilling, E. Jonsson, P. Kalvig, N. Charles, J. Tuduri, E. A. Deady, M. Sadeghi, H. Schiellerup, A. Müller, G. Bertrand, N. Arvanitidis, D. G. Eliopoulos, R.A. Shaw, K. Thrane, N. Keulen, Europe's rare earth element resource potential : An overview of REE metallogenetic provinces and their geodynamic setting, Ore Geol. Rev. 72 (2016) 838–856, https://doi.org/10.1016/j.oregeorev.2015.09.019.

[14] T. Pirom, A. Arponwichanop, U. Pancharoen, T. Yonezawa, S. Kheawhom, Yttrium (III) Recovery with D2EHPA in Pseudo-Emulsion Hollow Fiber Strip Dispersion System, Sci. Rep. 8 (2018) 1–11, https://doi.org/10.1038/s41598-018-25771-4.

[15] C. Tunsu, Hydrometallurgy in the recycling of spent NdFeB permanent magnets, 2018th ed., Elsevier Ltd, 2018. 10.1016/B978-0-08-102057-9.00008-1.

[16] M. Mohammadi, K. Forsberg, L. Kloo, J. Martinez, D. La Cruz, Å. Rasmuson, Hydrometallurgy Separation of ND (III), DY (III) and Y (III) by solvent extraction using D2EHPA and EHEHPA, Hydrometallurgy. 156 (2015) 215–224, https://doi.org/10.1016/j.hydromet.2015.05.004.

[17] T. Hatanaka, A. Matsugami, T. Nonaka, H. Takagi, F. Hayashi, T. Tani, N. Ishida, Rationally designed mineralization for selective recovery of the rare earth elements, Nat. Commun. 8 (2017) 1–10, https://doi.org/10.1038/ncomms15670.

[18] E. Polido Legaria, J. Rocha, C.W. Tai, V.G. Kessler, G.A. Seisenbaeva, Unusual seeding mechanism for enhanced performance in solid-phase magnetic extraction of Rare Earth Elements, Sci. Rep. 7 (2017) 1–13, https://doi.org/10.1038/srep43740.

[19] Y. Ding, D. Harvey, N.L. Wang, Two-zone ligand-assisted displacement chromatography for producing high-purity praseodymium, neodymium, and dysprosium with high yield and high productivity from crude mixtures derived from waste magnets, Green Chem. 22 (2020) 3769–3783, https://doi.org/10.1039/d0gc00495b.

[20] X. Du, T.E. Graedel, Global rare earth in-use stocks in NdFeB permanent magnets, J. Ind. Ecol. 15 (2011) 836–843, https://doi.org/10.1111/j.1530-9290.2011.00362.x.

[21] J.R. Peeters, E. Bracqguene, D. Nelen, M. Ueberschaar, K. Van Acker, J.R. Duflou, Forecasting the recycling potential based on waste analysis: A case study for recycling Nd-Fe-B magnets from hard disk drives, J. Clean. Prod. 175 (2018) 96–108, https://doi.org/10.1016/j.jclepro.2017.11.080.

[22] A. Lixandru, P. Venkatesan, C. Jönsson, I. Poenaru, B. Hall, Y. Yang, A. Walton, K. Güth, R. Gauß, O. Gutfleisch, Identification and recovery of rare-earth permanent magnets from waste electrical and electronic equipment, Waste Manag. 68 (2017) 482–489, https://doi.org/10.1016/j.wasman.2017.07.028.

[23] A. Kumari, M.K. Sinha, S. Pramanik, S.K. Sahu, Recovery of rare earths from spent NdFeB magnets of wind turbine: Leaching and kinetic aspects, Waste Manag. 75 (2018) 486–498, https://doi.org/10.1016/j.wasman.2018.01.033.

[24] E. Alonso, A.M. Sherman, T.J. Wallington, M.P. Everson, F.R. Field, R. Roth, R. E. Kirchain, Evaluating rare earth element availability: A case with revolutionary

demand from clean technologies, Environ. Sci. Technol. 46 (2012) 3406–3414, https://doi.org/10.1021/es203518d.

[25] Q. Tan, J. Li, X. Zeng, Rare Earth Elements Recovery from Waste Fluorescent Lamps: A Review, Crit. Rev. Environ. Sci. Technol. 45 (2015) 749–776, https://doi.org/10.1080/10643389.2014.900240.

[26] M. Gergoric, A. Barrier, T. Retegan, Recovery of Rare-Earth Elements from Neodymium Magnet Waste Using Glycolic, Maleic, and Ascorbic Acids Followed by Solvent Extraction, J. Sustain. Metall. 5 (2019) 85–96, https://doi.org/10.1007/s40831-018-0200-6.

[27] B. Liu, N. Zhu, Y. Li, P. Wu, Z. Dang, Y. Ke, Efficient recovery of rare earth elements from discarded NdFeB magnets, Process Saf. Environ. Prot. 124 (2019) 317–325, https://doi.org/10.1016/j.psep.2019.01.026.

[28] P. Venkatesan, Z.H.I. Sun, J. Sietsma, Y. Yang, An environmentally friendly electro-oxidative approach to recover valuable elements from NdFeB magnet waste, Sep. Purif. Technol. 191 (2018) 384–391, https://doi.org/10.1016/j.seppur.2017.09.053.

[29] P. Venkatesan, T. Vander Hoogerstraete, K. Binnemans, Z. Sun, J. Sietsma, Y. Yang, Selective Extraction of Rare-Earth Elements from NdFeB Magnets by a Room-Temperature Electrolysis Pretreatment Step, ACS Sustain. Chem. Eng. 6 (2018) 9375–9382, https://doi.org/10.1021/acssuschemeng.8b01707.

[30] S. Pavón, A. Fortuny, M.T. Coll, A.M. Sastre, Neodymium recovery from NdFeB magnet wastes using Primene 81R·Cyanex 572 IL by solvent extraction, J. Environ. Manage. 222 (2018) 359–367, https://doi.org/10.1016/j.jenvman.2018.05.054.

[31] N. Maât, V. Nachbaur, R. Lardé, J. Juraszek, J.M. Le Breton, An Innovative Process Using Only Water and Sodium Chloride for Recovering Rare Earth Elements from Nd-Fe-B Permanent Magnets Found in the Waste of Electrical and Electronic Equipment, ACS Sustain. Chem. Eng. 4 (2016) 6455–6462, https://doi.org/10.1021/acssuschemeng.6b01226.

[32] D. Dupont, K. Binnemans, Rare-earth recycling using a functionalized ionic liquid for the selective dissolution and revalorization of Y2O3:Eu3+ from lamp phosphor waste, Green Chem. 17 (2015) 856–868, https://doi.org/10.1039/C4GC02107J.

[33] M. Orefice, A. Eldosouky, I. Škulj, K. Binnemans, Removal of metallic coatings from rare-earth permanent magnets by solutions of bromine in organic solvents, RSC Adv. 9 (2019) 14910–14915, https://doi.org/10.1039/c9ra01696a.

[34] M.A.R. Önal, E. Aktan, C.R. Borra, B. Blanpain, T. Van Gerven, M. Guo, Recycling of NdFeB magnets using nitration, calcination and water leaching for REE recovery, Hydrometallurgy. 167 (2017) 115–123, https://doi.org/10.1016/j.hydromet.2016.11.006.

[35] S. Riaño, M. Petranikova, B. Onghena, T. Vander Hoogerstraete, D. Banerjee, M.R.S. Foreman, C. Ekberg, K. Binnemans, Separation of rare earths and other valuable metals from deep-eutectic solvents: A new alternative for the recycling of used NdFeB magnets, RSC Adv. 7 (2017) 32100–32113, https://doi.org/10.1039/c7ra06540j.

[36] M.V. Reimer, H.Y. Schenk-Mathes, M.F. Hoffmann, T. Elwert, Recycling Decisions in 2020, 2030, and 2040—When Can Substantial NdFeB Extraction Be Expected in the EU? Metals (Basel). 8 (2018) 867, https://doi.org/10.3390/met8110867.

[37] M. Sabbaghi, W. Cade, W. Olson, S. Behdad, The Global Flow of Hard Disk Drives: Quantifying the Concept of Value Leakage in E-waste Recovery Systems, J. Ind. Ecol. 23 (2019) 560–573, https://doi.org/10.1111/jiec.12765.

[38] A.B. Patil, V. Paetzel, R.P.W.J. Struis, C. Ludwig, Separation and Recycling Potential of Rare Earth Elements from Energy Systems: Feed and Economic Viability Review, Separations. 9 (2022) 1–15, https://doi.org/10.3390/separations9030056.

[39] A.B. Patil, P. Pathak, V.S. Shinde, S.V. Godbole, P.K. Mohapatra, Efficient solvent system containing malonamides in room temperature ionic liquids: Actinide extraction, fluorescence and radiolytic degradation studies, Dalt. Trans. 42 (2013) 1519–1529, https://doi.org/10.1039/c2dt32186f.

[40] D. Dupont, K. Binnemans, Recycling of rare earths from NdFeB magnets using a combined leaching/extraction system based on the acidity and thermomorphism of the ionic liquid [Hbet][Tf2N], Green Chem. 17 (2015) 2150–2163, https://doi.org/10.1039/c5gc00155b.

[41] Y. Wang, X. Guo, Y. Bi, J. Su, W. Kong, X. Sun, Enrichment of trace rare earth elements from the leaching liquor of ion-absorption minerals using a solid complex centrifugal separation process, Green Chem. 20 (2018) 1998–2006, https://doi.org/10.1039/c7gc03674d.

[42] R. Boyd, L. Jin, P. Nockemann, P.K.J. Robertson, L. Stella, R. Ruhela, K.R. Seddon, H.Q.N. Gunaratne, Ionic liquids tethered to a preorganised 1,2-diamide motif for extraction of lanthanides, Green Chem. 21 (2019) 2583–2588, https://doi.org/10.1039/c9gc00089e.

[43] K. Wang, H. Adidharma, M. Radosz, P. Wan, X. Xu, C.K. Russell, H. Tian, M. Fan, J. Yu, Recovery of rare earth elements with ionic liquids, Green Chem. 19 (2017) 4469–4493, https://doi.org/10.1039/c7gc02141k.

[44] N. Kumari, P.N. Pathak, P.K. Mohapatra, Comparative evaluation of different extractants toward cloud formation behavior and metal ion extraction: Spectrophotometric, dynamic light scattering, and extraction studies, Ind. Eng. Chem. Res. 52 (2013) 15146–15153, https://doi.org/10.1021/ie401658c.

[45] E. Tatara, K. Materna, A. Schaadt, H.J. Bart, J. Szymanowski, Cloud point extraction of Direct Yellow, Environ. Sci. Technol. 39 (2005) 3110–3115, https://doi.org/10.1021/es049381x.

[46] A. Ohashi, T. Hashimoto, H. Imura, K. Ohashi, Cloud point extraction equilibrium of lanthanum(III), europium(III) and lutetium(III) using di(2-ethylhexyl) phosphoric acid and Triton X-100, Talanta. 73 (2007) 893–898, https://doi.org/10.1016/j.talanta.2007.05.012.

[47] J. Elistratova, A. Mustafina, A. Litvinov, V. Burilov, A. Khisametdinova, V. Morozov, R. Amirov, Y. Burilova, D. Tatarinov, M. Kadirov, V. Mironov, A. Konovalov, The effect of temperature induced phase transitions in aqueous solutions of triblock copolymers and Triton X-100 on the EPR, magnetic relaxation and luminescent characteristics of Gd(III) and Eu(III) ions, Colloids Surfaces A Physicochem. Eng. Asp. 422 (2013) 126–135, https://doi.org/10.1016/j.colsurfa.2012.12.023.

[48] N. De Jong, M. Draye, A. Favre-Réguillon, G. LeBuzit, G. Cote, J. Foos, Lanthanum (III) and gadolinium(III) separation by cloud point extraction, J. Colloid Interface Sci. 291 (2005) 303–306, https://doi.org/10.1016/j.jcis.2005.07.004.

[49] T. Suoranta, O. Zugazua, M. Niemelä, P. Perämäki, Recovery of palladium, platinum, rhodium and ruthenium from catalyst materials using microwave-assisted leaching and cloud point extraction, Hydrometallurgy. 154 (2015) 56–62, https://doi.org/10.1016/j.hydromet.2015.03.014.

[50] H. Liang, Q. Chen, C. Xu, X. Shen, Selective cloud point extraction of uranium from thorium and lanthanides using Cyanex 301 as extractant, Sep. Purif. Technol. 210 (2019) 835–842, https://doi.org/10.1016/j.seppur.2018.08.071.

[51] F.H. Quina, W.L. Hinze, Surfactant-mediated cloud point extractions: An environmentally benign alternative separation approach, Ind. Eng. Chem. Res. 38 (1999) 4150–4168, https://doi.org/10.1021/ie980389n.

[52] A. Mustafina, L. Zakharova, J. Elistratova, J. Kudryashova, S. Soloveva, A. Garusov, I. Antipin, A. Konovalov, Solution behavior of mixed systems based on novel amphiphilic cyclophanes and Triton X100: Aggregation, cloud point phenomenon and cloud point extraction of lanthanide ions, J. Colloid Interface Sci. 346 (2010) 405–413, https://doi.org/10.1016/j.jcis.2010.03.002.

[53] X. Li, N. Song, W. Feng, Q. Jia, Cloud point extraction of rare earths and zinc using 1,10-phenanthroline and Triton X-114 coupled with microwave plasma torch-atomic emission spectrometry, Anal. Methods. 9 (2017) 5333–5338, https://doi.org/10.1039/c7ay00421d.

[54] C. Labrecque, D. Larivière, Quantification of rare earth elements using cloud point extraction with diglycolamide and ICP-MS for environmental analysis, Anal. Methods. 6 (2014) 9291–9298, https://doi.org/10.1039/c4ay01911c.

[55] A.B. Patil, V.S. Shinde, P.N. Pathak, P.K. Mohapatra, V.K. Manchanda, Modified synthesis scheme for N, N'-dimethyl-N, N'-dioctyl-2, (2'- hexyloxyethyl) malonamide (DMDOHEMA) and its comparison with proposed solvents for actinide partitioning, Radiochim. Acta. 101 (2013) 93–100, https://doi.org/10.1524/RACT.2013.1998.

[56] S. Kori, Cloud point extraction coupled with back extraction: a green methodology in analytical chemistry, Forensic Sci. Res. 6 (2021) 19–33, https://doi.org/10.1080/20961790.2019.1643567.

[57] N. Kumari, P.K. Verma, P.N. Pathak, A. Gupta, A. Ballal, V.K. Aswal, P.K. Mohapatra, Extractant mediated nano-aggregate formation in Triton X-114 aided cloud formation: structural insights from TEM and SANS studies, RSC Adv. 5 (2015) 95613–95617, https://doi.org/10.1039/c5ra18546g.

[58] R.J. Ellis, Acid-switched Eu(III) coordination inside reverse aggregates: Insights into a synergistic liquid-liquid extraction system, Inorganica Chim. Acta. 460 (2017) 159–164, https://doi.org/10.1016/j.ica.2016.08.008.

[59] R.R. Zairov, A.R. Mustafina, R.R. Amirov, L.M. Pilishkina, I.S. Antipin, A.I. Konovalov, Extraction of Lanthanum and Gadolinium (III) at the Cloud Point Using p-Sulfonatocalyx [n] arenes as Chelating Agents, Colloid J. 71 (2009) 69–75, https://doi.org/10.1134/S1061933X09010086.

[60] Z. Li, A. Kedous-Lebouc, J.M. Dubus, L. Garbuio, S. Personnaz, Direct reuse strategies of rare earth permanent magnets for PM electrical machines-an overview study, EPJ Appl. Phys. 86 (2019) 1–10, https://doi.org/10.1051/epjap/2019180289.